IEEE Access
Multidisciplinary ⋮ Rapid Review ⋮ Open Access Journal

Received 5 May 2023, accepted 20 May 2023, date of publication 24 May 2023, date of current version 13 June 2023.

Digital Object Identifier 10.1109/ACCESS.2023.3279499

RESEARCH ARTICLE

Use of the Thermal Inertia of Trains for Contributing to Primary Frequency Control and Inertia of Electric Power Systems

JESÚS ARAÚZ [1,2,3] AND SERGIO MARTINEZ [1], (Senior Member, IEEE)

[1]Escuela Técnica Superior de Ingenieros Industriales, Universidad Politécnica de Madrid, 28006 Madrid, Spain
[2]Panama Railway Engineering Research Group, Faculty of Electrical Engineering, Universidad Tecnológica de Panamá, Panama City 0819-07289, Panama
[3]Research Group Energy and Comfort in Bioclimatic Buildings, Faculty of Mechanical Engineering, Universidad Tecnológica de Panamá, Panama City 0819-07289, Panama

Corresponding author: Jesús Araúz (jesus.arauz@alumnos.upm.es)

This work was supported in part by the Panamanian Institution Secretaría Nacional de Ciencia, Tecnología e Innovación (SENACYT), under Grant 270-2022-107; and in part by the Spanish National Research Agency Agencia Estatal de Investigación, under Grant PID2019-108966RB-I00 /AEI/ 10.13039/501100011033.

ABSTRACT The current trend of massively incorporating renewable-based generation into power systems is affecting frequency stability. This generation does not inherently provide inertia owing to its electronic interface. Therefore, many approaches have been proposed to address the problem of inertia weakening. Beyond the new trends of making new generation and storage responsive to grid needs, this study addresses the problem from the role of consumers. The use of railway consumption to contribute to frequency control tasks, without affecting train circulation, is proposed. For the first time, the provision of virtual inertia combined with primary frequency control is presented. This is achieved by means of the power consumption of ventilation and air conditioning systems, while maintaining the thermal comfort of passengers. To illustrate this new concept, a case study of a real metro line is presented. The results demonstrate the benefits of using the thermal inertia of trains to contribute to grid frequency control. Also, some insights into technical requirements and possible issues are provided. An appropriate combination of primary frequency control and virtual inertia can reduce technical requirements and provide better frequency performance.

INDEX TERMS Frequency control, virtual inertia, railways, demand response, thermal comfort.

I. INTRODUCTION

Due to efforts to reduce climate change, power systems have been facing successive changes in their structures, operation, and technical requirements. Toward a system with low emissions, technological developments are oriented to the integration of renewable energy-based generation. Likewise, in addition to distributed generation, different types of storage systems, loads, and electrical and communication networks are being integrated. This implies new challenges, one of them being the maintenance of stability, safety, and reliability of power systems [1].

The participation of emerging generating technologies implies integrating many electronic converters into the power system. These displace some conventional power plants and must operate in harmony with the rest. In addition, the deployment of smart grids is also based on electronic converters. However, electronic converters do not intrinsically provide several ancillary services (voltage regulation, power-frequency control, fault response, etc.). Among these, frequency control is attracting research interest due to the reduction of power systems inertia and to the active power fluctuations of renewable generation, such as solar and wind power [2].

Consequently, many authors have focused their research on the provision of frequency control by renewable energy-based power plants. For example, Ramesh et al. [3] made a detailed review of frequency control in systems based on solar and wind energy, provided a systematic summary of the possible lines of research, and proposed a control capable of handling primary and secondary regulation, and virtual inertia. Piero et al. [4] proposed a structure for flexible

The associate editor coordinating the review of this manuscript and approving it for publication was Diego Bellan.

photovoltaic generation based on power curtailment, and on storage operated as secondary reserve. Padhy and Panda [5] proposed a new optimization tool for frequency control in systems with distributed generation, consumption, and storage, where better performance is achieved in regulation tasks compared to other controls and optimizers. Rezk et al. [6] presented a new optimization algorithm to determine the optimal gains of secondary frequency controllers in a two-zone system with thermal, hydroelectric, wind, and solar generation.

Apart from power plants, other participants of power systems can also contribute to ancillary services. This contribution is included in the demand response concept. Particularly, consumers can collaborate in frequency control tasks [7], [8].

In a previous work [9], the authors reviewed some of the recent trends in frequency control based on demand management. In addition, the participation of railways in primary frequency control tasks is studied, based on the variation of the power consumption of the air conditioning system of trains, without affecting the thermal comfort of passengers. This was done by modeling the electrical power system by the oscillation equation, and the railway system by train kinematics and thermal characteristics. The thermal model was limited to a second order one to consider the thermal inertia of air and mass of trains. The air conditioning model determines the thermal power needed to maintain the thermal comfort. They limited the work to studying the contribution of trains to primary frequency control considering the train thermal envelope characteristics.

The present work uses the same modeling methodology, but with the aim of assessing the possible contribution of trains to the inertia of the electric power system and its combination with primary control to enhance frequency behavior. In literature, there are few studies related to the development of virtual inertia [10] by loads. Among others: Fang et al. [11] reviewed several techniques for improving the inertia of power systems by means of virtual inertia, where the feasible participation of DC links, batteries, and ultracapacitors was remarked; Chen et al. [12] analyzed the possibilities of virtual inertia contribution by ''smart loads'', that can operate at different voltage values, as long as the voltage operation range is not infringed; Yang et al. [13] also implemented ''smart loads'' with a very similar topology to [12], but focused on the mitigation of voltage fluctuations in a DC microgrid with renewable generation, storage systems, and critical loads.

However, it is significant the little amount of research related to how the railway sector could provide inertia to electrical power systems. In [9], the authors observed the absence of studies on the contribution to primary frequency control. For the present work, only two papers related to virtual inertia provision were found: Hao and Chen [14] proposed an improved algorithm for the emulation of inertia by a bidirectional converter in the catenary of a direct current railway, in which voltage fluctuations were reduced by means of a virtual capacitor; and Yu et al. [15] proposed a novel control, based on virtual inertia, to mitigate low-frequency oscillations usually present in high-speed AC railways, where a virtual capacitor is also emulated to mitigate voltage fluctuations in the DC link on board the train, which also reduces low-frequency oscillations in the catenary. In both cases, virtual inertia is applied to the mitigation of voltage fluctuations, but not to power system frequency control.

The main contributions of this work are: the identification of this research gap; the proposal of contributing to fill this gap with the provision of inertia from railway systems, individually and together with primary frequency control; and the proposal of one possible approach to achieve it by using some train auxiliary consumptions. The latter is complemented with an assessment of the virtual inertia that heating, ventilation, and air conditioning (HVAC) systems onboard could provide to the grid, without compromising the thermal comfort of passengers. This evaluation allows estimating the possible benefits that the grid could receive from railway systems, but also allows knowing the technical capabilities of HVAC systems to achieve a certain level of contribution.

The article is structured as follows: section II contains the explanation of the modeling of electrical and railway systems, aimed at evaluating the frequency deviations of the grid and their relation to controllers aggressivity; section III presents a case study inspired by the operational characteristics of a real train; section IV shows the results of the case study, where the combinations of controllers and power system events are considered, and a statistical study; and section V exposes the main conclusions.

II. METHODOLOGY

The evaluation of the contribution of trains to the inertia of electric power systems requires considering the frequency behavior of grids and the railway performance. For this, it is necessary to model both systems coherently. Electric power systems can be modeled with different levels of detail, as can be seen in Ochoa and Martinez [16], where the primary frequency control is studied with two models based on power flows and on the oscillation equation, respectively. Similarly, railway systems, depending on the traction technology and the electrification configuration, can be modeled with different approaches [17], [18], [19], [20], [21], [22], [23], which will depend on the nature of the study (dynamic, mechanical, electrical, electronical, etc.). In this work, the same modeling approach the authors presented in [9] is used (Fig. 1). Apart from modeling details, a statistical analysis of temperature, frequency, and power is done to gain insights into the efficiency and technical requirements of the contribution of railways to frequency control.

A. RAILWAY SYSTEM

For the aim of this work, to achieve participation of trains in grid frequency control tasks, it is appropriate to describe the

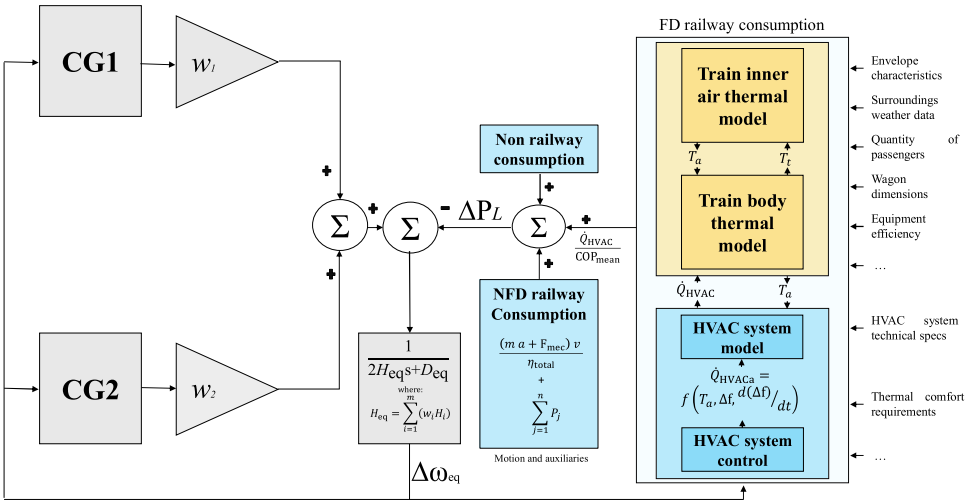

FIGURE 1. Schematic representation of modeling. CG: conventional generation. (N)FD: (Non) Frequency dependent.

railway system electrically, but in response to instantaneous dynamic requirements. This implies considering the resulting energy directly dependent on traction as the center of the modeling. Also, railway power estimation must consider the dynamics of the auxiliary systems, specifically the HVAC system.

1) ROLLING STOCK AND CATENARY MODELING

Given the objectives of this analysis, it is acceptable to ignore some very specific dynamics of railways, such as: pantograph-catenary interaction, wheel-rail interaction, joints between cars, catenary thermal effects due to load variations and environmental temperatures, etc. Each train is described as a controlled current source where the imposed current will depend on the instantaneous voltage of the catenary and the instantaneous electrical power required ($P_{\text{elect total}}$). In the following equations: m is the mass of the train, a is its acceleration, F_{mec} is the movement resistance force, v is the speed of train, η_{total} is the total power efficiency from catenary to wheels, P_{aux} is the auxiliary power consumption (HVAC, lights, communications, etc.), F_{aero} is the aerodynamic component of movement resistance force, A is an aerodynamic coefficient related to mass, B is an aerodynamic coefficient related to the involved stiffness of the train, C is an aerodynamic coefficient related to the aerodynamic profile of the train parts, F_{slope} is the component of movement resistance force imposed by the slope of railway layout, g is the gravity acceleration, $\text{ang}_{\text{slope}}$ is the slope of railway layout, F_{curve} is the component of movement resistance force imposed by railway layout curvature, R is the radius of curvature, L_{train} is the length of the train, ang_d is the deflection angle, F_{tunnel} is the component of movement resistance force of running through tunnels, L_{tunnel} is the length of tunnels, $\dot{Q}_{\text{HVAC}}$ is the heat power output of the HVAC system, COP_{mean} is the average coefficient of performance of the HVAC system, P_j is the j^{th} power consumed by the n auxiliary consumptions, $\dot{V}$ is the flow of air injected by the HVAC system, ρ is the density of the injected air, C_p is the specific heat at constant pressure of the injected air, and ΔT is the temperature difference between the injected air and the air inside the trains.

$$P_{\text{elect total}} = \frac{(ma + F_{\text{mec}})\, v}{\eta_{\text{total}}} + P_{\text{aux}} \tag{1}$$

$$F_{\text{aero}} = A + Bv + Cv^2 \tag{2}$$

$$F_{\text{slope}} = mg \sin(\text{ang}_{\text{slope}}) \tag{3}$$

$$F_{\text{curve}} = \begin{cases} \dfrac{0.6\, mg}{R}, & R \le L_{\text{train}} \\ \dfrac{0.0105\, mg(\text{ang}_d)}{L_{\text{train}}}, & R > L_{\text{train}} \end{cases} \tag{4}$$

$$F_{\text{tunnel}} = 1.3 \times 10^{-7} mgL_{\text{tunnel}} \tag{5}$$

$$P_{\text{aux}} = \frac{\dot{Q}_{\text{HVAC}}}{\text{COP}_{\text{mean}}} + \sum_{j=1}^{n} P_j, \dot{Q}_{\text{HVAC}} = \dot{V}\rho C_p \Delta T \tag{6}$$

The electrification system can be represented as a circuit made up of the catenary, rails, and traction substations. The catenary, which includes all the conductors involved (feeders, return, etc.), is represented by impedances, as well as the rails. Traction substations, which may be previously supplied by an internal railway circuit or directly by a distribution grid, are represented as voltage sources at catenary voltage. Depending on the type of supply (AC or DC), the topologies of substations, the connectivity between catenary sections, the inductive and capacitive terms, and the direction of power flow in the substations, the model adjustment may vary. However, the system coupling variable with the electric power system is the total railway power. This allows to omit certain details during implementation.

2) THERMAL MODELING

The need for a thermal model of trains lays on modeling the technical requirements and dynamics of HVAC systems.

These systems respond to the resulting heat flows in the trains and to frequency deviations, but subject to thermal comfort restrictions. There are several works on the thermal modeling of trains [24], [25], [26], [27], [28], [29], [30], [31], where extensive discretizations are made to represent each component of the envelope in great detail. These studies are aimed at evaluating the thermal comfort and/or the thermodynamics of trains, internally and externally. According to the scope of this work, the model in [9] is used, which uses some approximations made in [31]. Equations (7) and (8) are used to represent the thermodynamics of trains by a second order system with one-dimensional heat flow. Equation (7) represents the dynamics of the inner air temperature of trains, where TM_a represents the thermal mass of the air, T_a is the air temperature, $\dot{Q}_{\mathrm{mix1}}$ is the global thermal power load seen by inner air (people, radiation through windows, infiltrations, etc.), $U_{\mathrm{ao}}\ A_{\mathrm{ao}}$ is the product of the thermal transmittance between the indoor and outdoor air times the surface involved, T_o is the temperature of the outdoor air, $U_{\mathrm{at}}\ A_{\mathrm{at}}$ is the product of the thermal transmittance between the interior air and the body of the train times the surface involved, TM_t is the train body thermal mass, T_t is the train body temperature, and $\dot{Q}_{\mathrm{mix2}}$ is the total thermal power load seen by the body of the train. The following equations describe lumped systems. The air heat equation and the train body equation assume that all the air in the train is lumped at a single point, as the mass of the train is. In addition, all those masses that do not have enough thermal mass to be considered as individual systems can be added to the two mentioned systems.

$$\mathrm{TM}_a \frac{dT_a}{dt} = \dot{Q}_{\mathrm{mix1}} + U_{\mathrm{ao}}A_{\mathrm{ao}}\left(T_o - T_a\right) + U_{\mathrm{at}}A_{\mathrm{at}}\left(T_t - T_a\right) - \dot{Q}_{\mathrm{HVAC}} \tag{7}$$

$$\mathrm{TM}_t \frac{dT_t}{dt} = \dot{Q}_{\mathrm{mix2}} - U_{\mathrm{at}}A_{\mathrm{at}}\left(T_t - T_a\right) \tag{8}$$

Among the terms mentioned, the thermal power of the HVAC system is the one which is usually controlled to adjust the thermal state of trains. Equation (6) represents a simplified model, which only considers the HVAC system as the air flow injected into wagons. This can be modeled in different ways, depending on whether its operation is through an on/off logic [32] or a variable frequency drive [33], [34], [35]. The latter allows to adjust continuously the thermal power by altering the speed of motors. This indirectly affects each of the terms in (6). Depending on the HVAC system used, the terms can be controlled individually or together for power tracking. In this work, it is done as in [9], where there is a proportional integral controller to act on $\dot{V}$ and, separately, the operating temperature is linearly adjusted to provide primary frequency control. Due to the scope of the model, altering the setpoint temperature, or any other implicit or explicit factor in equation (6), is mathematically equivalent to computing another power term. Thus, (6) can be rewritten as (9). Likewise, a similar equivalence can be obtained if it is decided to modify the injected air flow for an identical follow-up of power, as shown in (10). In these equations, the terms with an asterisk $(*)$ represent the alteration of parameters by some specific control. The quantities $\dot{Q}_{\mathrm{HVAC1}}$ and $\dot{Q}_{\mathrm{HVAC2}}$ represent the power added to the normal operation of the HVAC system to fulfill a desired output.

$$\dot{Q}_{\mathrm{HVAC}} = \dot{V}\rho C_p\left(\Delta\mathrm{T} + \Delta\mathrm{T}^*\right) = \dot{V}\rho C_p\Delta\mathrm{T} + \dot{V}\rho C_p\Delta\mathrm{T}^* = \dot{V}\rho C_p\Delta\mathrm{T} + \dot{Q}_{\mathrm{HVAC1}} \tag{9}$$

$$\dot{Q}_{\mathrm{HVAC}} = \left(\dot{V} + \dot{V}^*\right)\rho C_p\Delta\mathrm{T} = \dot{V}\rho C_p\Delta\mathrm{T} + \dot{V}^*\rho C_p\Delta\mathrm{T} = \dot{V}\rho C_p\Delta\mathrm{T} + \dot{Q}_{\mathrm{HVAC2}} \tag{10}$$

Therefore, in the present work a simplified model of the HVAC system and its control is used, where the dynamics of its individual components is considered in an aggregated form. Some works do describe each of the components of the HVAC thermodynamic cycle [34], but this level of detail is not needed for estimating the HVAC system contribution to frequency control tasks. Of course, if the interest were on each element thermal behavior, more detailed studies could be done by considering the disaggregated individual dynamics of each component, as in [36]. Then, deeper insights and/or different results on HVAC system frequency control can be obtained.

The added power term ($\dot{Q}_{\mathrm{HVACa}}$) varies proportionally to frequency deviations and its derivative to provide primary control and virtual inertia [10], [12], [13], [37], [38], respectively. Equation (11) shows the computation of the added power, where Δf is the frequency deviation, D_p is a term that relates the HVAC system power variation to frequency deviations, D_v is a term that relates the HVAC system power variation to the derivative of frequency deviations, and K_p and K_v are coefficients for adjusting the sensitivity of primary control and virtual inertia, respectively. Mathematically, K_p and K_v can also be used to limit the contribution of each of the controls, making it easier to evaluate their combinations.

$$\dot{Q}_{\mathrm{HVACa}} = \Delta f D_p K_p + \frac{d\,\Delta f}{dt} D_v K_v \tag{11}$$

It is important to clarify that (11) is valid for HVAC systems in cooling and heating mode. If there is a positive frequency deviation (frequency increase) the control indicates that the thermal power must be increased. If there is a decrease, it should be decreased. In heating, this would represent that the heat injection must be increased or decreased, respectively. In cooling, it would represent the same, but injecting more or less cold air, respectively. The injection of hot or cold air is proportionally linked to electrical power consumption, which is the magnitude that influences frequency deviations.

B. ELECTRIC POWER SYSTEM

In order to study grid frequency deviations, the model based on frequency control used in [9] is adopted. This type of model has been widely used in literature, both for the study of the integration of renewable energies into the electricity

grid [5], [6], [39] and for the evaluation of the possibilities of demand response (electric vehicles [40], refrigeration centers [41], etc.). Equation (12) represents the relation between frequency deviations and power deviations on a power system with m power plants, where: $\Delta\omega_{\text{eq}}$ represents the equivalent frequency deviations of the system, ΔP_L is the power deviations seen by the grid, w_i is the participation factor of the i^{th} generator into energy dispatch, H_i is the inertia of the i^{th} generator, $D_i(s)$ is the transfer function that represents the dynamics of the i^{th} generator, $S_i(s)$ is the transfer function that represents the dynamics of the speed controller of the i^{th} generator, and s is the Laplace operator.

$$\frac{\Delta\omega_{\text{eq}}(s)}{\Delta P_L(s)} = \frac{-1}{2\left(\sum_{i=1}^{m} w_i H_i\right)s + D_{\text{eq}} + \sum_{i=1}^{m} w_i D_i(s) S_i(s)} \tag{12}$$

The resulting load profile of the railway system under study is considered as the load that normally produces frequency deviations (ΔP_L). Also, ΔP_L can represent load events. The participation of railways in frequency control can also be taken into account by means of ΔP_L. This is possible by adjusting the instantaneous consumption of the HVAC system of trains, defined by (12) and (11). Then, the HVAC system consumption depends on thermal comfort and on grid frequency behavior. By using (11), it is possible to emulate power profiles similar to those from conventional generators under frequency deviations. The contribution of a conventional generator is showed in (12), where it reacts to frequency deviation and its derivative through its speed controller ($S_i(s)$) and its inertia (H_i), respectively.

III. CASE STUDY

To illustrate the possibilities of contribution of trains, a case study based on Panama Metro Line 1 (PML1) is considered in this section. The same general characteristics showed in [9] are used (see appendix for further details), where a railway system powered by direct current is partially modeled. This contemplates a circulation of four trains, on two tracks, through three traction stations, and five passenger stations (the reader is suggested to review the previously commented article to see the specific characteristics of the model, as well as the speed profiles). However, in this occasion the operating limits of the real ventilation and air conditioning (VAC) system is considered, as well as the environmental and load conditions used in the PML1 sizing.

According to the managing company of PML1, the trains have four tractor wagons and one non-tractor wagon. Two electronic converters are installed in the non-tractor wagon to drive, mainly, the VAC units installed in the train. The two electronic converters have a total estimated capacity of 484 kW with a minimum load limit of 96.8 kW. Each wagon has two VAC units with a cooling capacity of 38 kW. Therefore, the total train has a cooling capacity of 380 kW. As the entire air mass and the body of the train are being considered lumped at a single point, the physical distribution of the VAC system is not considered. This implies that all the thermal power involved is grouped in the $\dot{Q}_{\text{HVAC}}$ term of (7).

To determine the values of D_p and D_v of (11), an iterative method is used. It starts from considering the maximum power of the VAC system and frequency limits. After obtaining the initial values, they are varied until determining the point where the thermal capacity of the VAC system is exceeded. Finally, the aggressiveness of each one, individually and/or collectively, is adjusted by means of k_p and k_v to analyze the response of the control. It should be noted that, for this case study, the initial values of terms were calculated as follows: $D_p = \dot{Q}_{\text{max}}/\Delta f_{\text{max}}$ and $D_v = \dot{Q}_{\text{max}}/\text{ROCOF}_{\text{max}}$, where $\dot{Q}_{\text{max}}$ is the maximum heat power developable and $\text{ROCOF}_{\text{max}}$ is the maximum rate of change of frequency (ROCOF) allowable. D_p and D_v can also be calculated by applying optimization algorithms to find the best values according to an objective [6], but this is not strictly needed for assessing the train HVAC system contribution to frequency control tasks.

According to the regulations considered [42], the maximum acceptable frequency deviation is $\pm$ 0.8 Hz. The absolute ROCOF is usually limited between 0.1 Hz/s and 1.0 Hz/s [43]. Based on the results observed in [9], a maximum allowable deviation of $\pm$ 0.1 Hz/s is selected. These limits, along with the maximum available thermal power, 380 kW, provide the values of D_p and D_v. Initially, these are 475 kW/Hz and 3800 kWs/Hz. After iterating, it is found that the first values that provide the maximum thermal power are 2020 kW/Hz and 551 kWs/Hz.

It is worth mentioning that the applied iteration method is going to be used in the next case studies. Although droop coefficients relate power to frequency, this control shares the same topology as the one in [9]. Therefore, the control strategy and its stability margins have already been tested under acceptable VAC system operation ranges. The decrease of gain margin due to the increase of frequency control gains is also shown in [9]. In the present work, gain values are chosen according to this and based on real VAC system requirement, avoiding its saturation.

The electric power system is modeled as in [9], a 60 Hz system with two hydroelectric plants. These provide the total energy supply and primary and secondary frequency control. Both plants have an inertia constant of 4.0 s and a power capacity of 1.0 p.u. at a base power of 180 MW. In addition, a load damping factor of 1% is used. The model is able to easily simulate sudden load or generation loss events.

Finally, two general scenarios are studied: sudden loss of load and sudden loss of generation. The first one studies a loss of an equivalent load of 0.1 p.u. The second studies a loss of a generation plant of 0.1 p.u. and an inertia constant of 2.0 s. Each general scenario considers three possible cases: primary control, virtual inertia, and primary control combined with virtual inertia. In the first two cases, K_p and K_v are varied from 0% to 100% in intervals of 20%. In the latter case, the two controls are combined in the following proportions:

(K_p, K_v) = (0.8, 0.2); (0.6, 0.4); (0.4, 0.6); (0.2, 0.8); (1, 1), where the contribution of each control is also limited to half the remaining capacity of the VAC system. That is, the power available after generating the thermal power setpoint exclusively based on (6).

IV. RESULTS

The realization of models and the development of case studies are carried out in Matlab/Simulink, in discrete mode with a sampling period of 0.25 cycles of 60 Hz. For the model of the railway system in direct current, the tools of the *Specialized Power Systems* library are used, but for the electric power system, and its coupling to railway model, conventional Simulink blocks are used.

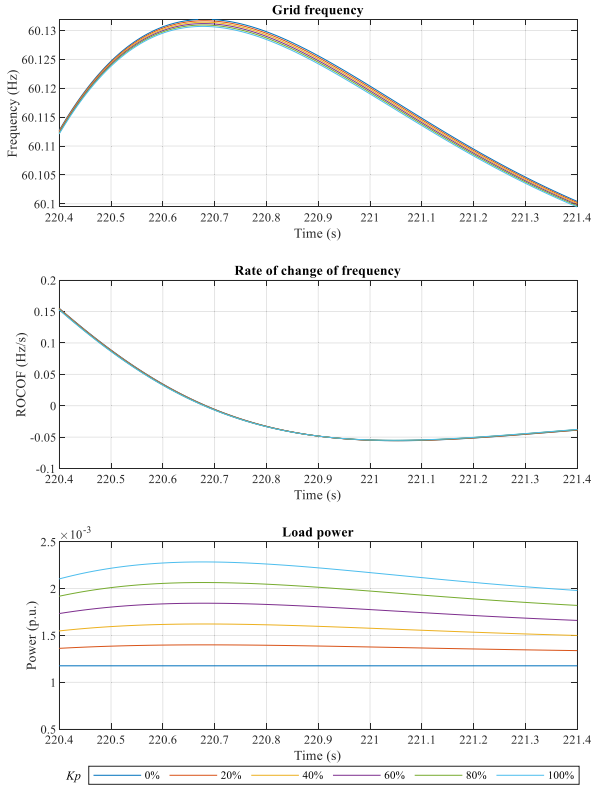

FIGURE 2. Load frequency control responses following a load shedding under different control aggressivity. Primary frequency control.

A. CASE STUDY 1. NON-RAILWAY CONSUMPTION. RESPONSE TO A SUDDEN LOAD SHEDDING

In the first place, a general case study is presented without considering the disturbance in the grid caused by the railway system. In other words, the same model is used, but without including railway consumption. A load with the same capacity of the two electronic converters of the PML1 trains is considered. It operates at half capacity, and it has the possibility of providing primary frequency control and virtual inertia by means of (11). As in the previous section, the terms D_p and D_v are determined first. These are calculated based on the available power band, i.e., 0.0012 p.u., and the frequency and variation rate limits considered. Finally, different values of K_p and K_v are considered to evaluate the behavior.

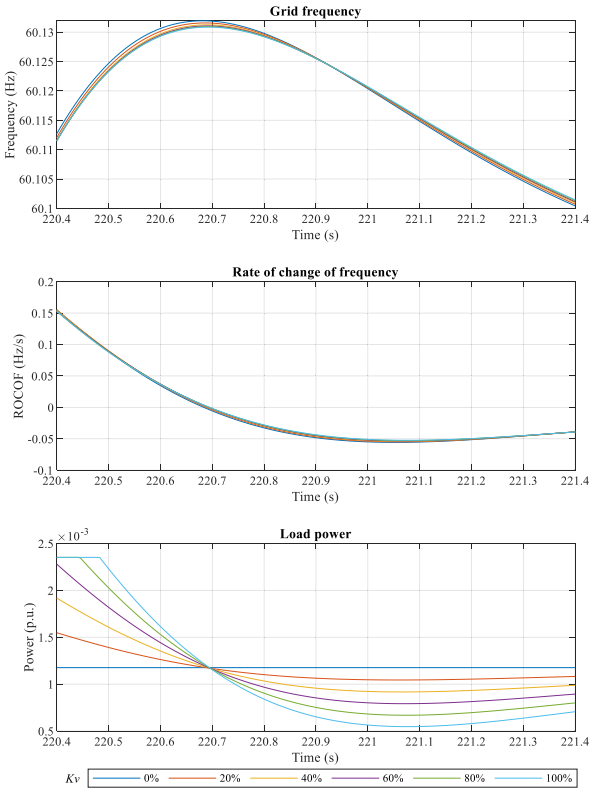

FIGURE 3. Load frequency control responses following a load shedding under different control aggressivity. Virtual inertia.

Fig. 2 and Fig. 3 show the evolution of frequency, ROCOF, and load power after a sudden load shedding of 0.1 p.u. Fig. 2 shows the results with just primary frequency control, and Fig. 3 with just virtual inertia. On the one hand, the results of the primary control share similarities with the results of [9] and [44], where higher gains result in higher power consumption from the controlled load and, therefore, better frequency control. Furthermore, it is noticeable that the ROCOF does not change appreciably. On the other hand, the virtual inertia is configured to reduce the ROCOF, which also impacts on frequency deviations. It is worth mentioning that, as the part of the power involved in the control is just a small fraction (0.26%) of the power of the whole electric system, the impact of the proposed control can not be easily appreciated with the scale used in Fig. 2 and Fig. 3. However, this scale allows to show the overall behavior. For example, the maximum frequency deviation can be clearly identified around $t = 220.7$ s.

To better appreciate the details, Fig. 4 and Fig. 5 use the same results of Fig. 2 and Fig. 3, but showing the deviations from the reference case. I.e., the values of the case without frequency control have been subtracted from those of each case with frequency control. Every negative value seen in Fig. 4 and Fig. 5 represents a reduction, while positive ones

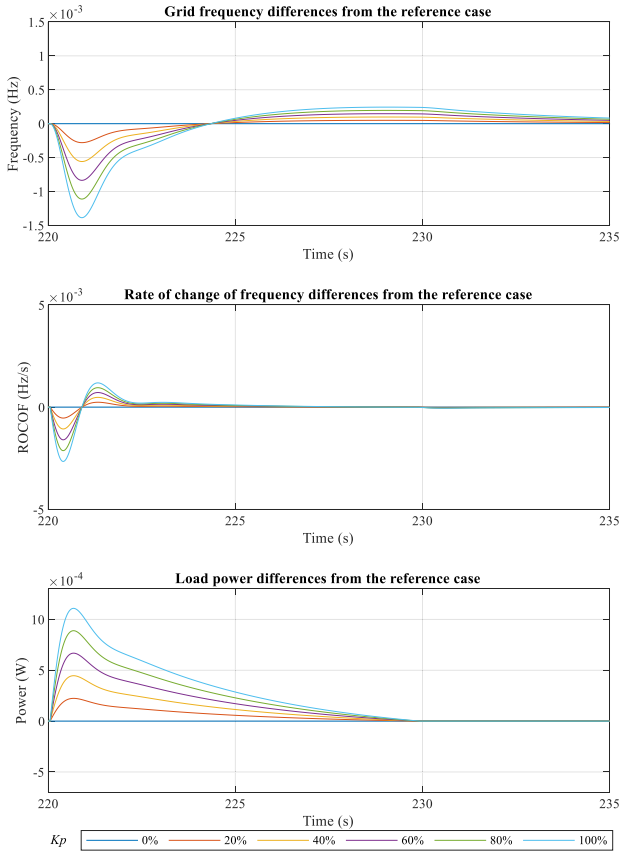

FIGURE 4. Load frequency control responses following a load shedding under different control aggressivity. The reference case (without frequency control) has been subtracted from each case. Primary frequency control.

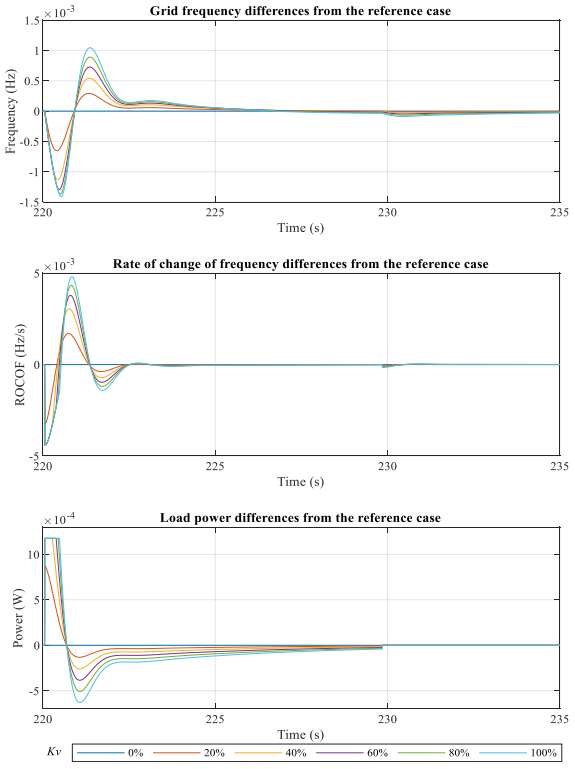

FIGURE 5. Load frequency control responses following a load shedding under different control aggressivity. The reference case (without frequency control) has been subtracted from each case. Virtual inertia.

stand for increases. The trivial case (blue horizontal line) is kept just for reference purposes. This way, it is easier to notice the effects of both controls. Primary frequency control (Fig. 4) mainly impacts on frequency deviations and on the amplitude of load power variations. On the contrary, virtual inertia (Fig. 5) mainly impacts on ROCOF and on load power fluctuations. Primary frequency control provides longer frequency reductions (first row) and power increases (third row) than virtual inertia. Virtual inertia slows down frequency variation faster than primary frequency control (second row) but requires higher power fluctuation than primary control (third row).

It is worth mentioning that positive differences at frequency deviations and variations, which mean worsening in the load shedding scenario considered, are found at some moments. However, the presence of the negative differences, which mean improvement in this scenario, takes place at the most important moments: around the maximum frequency deviation (about $t = 220.7$ s), in the case of primary frequency control, and just after the disturbance, in the case of virtual inertia. In addition, higher aggressivity improves the behavior in both cases, but it can saturate the action of VAC systems faster, apart from temporary deteriorate frequency performance in some instants.

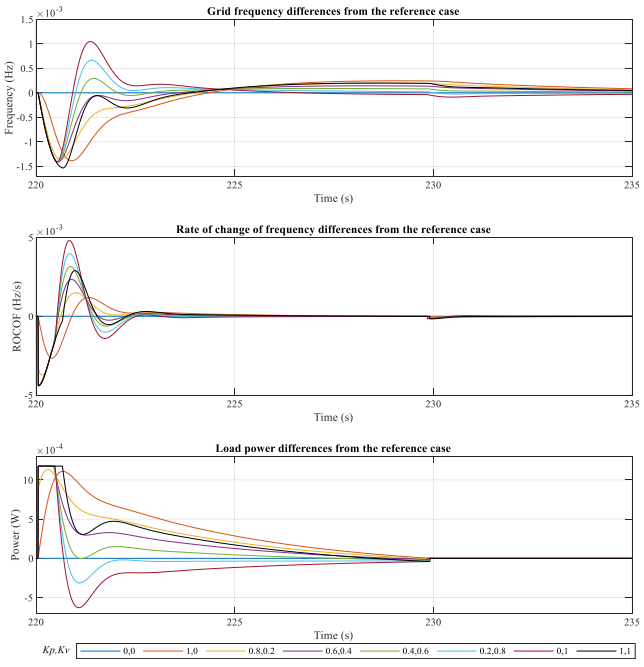

FIGURE 6. Combination of primary frequency control and virtual inertia. The reference case (without frequency control) has been subtracted from each case.

Fig. 6 shows the results of combining both controls, where each curve corresponds to a pair (K_p, K_v). Likewise, those controls with more aggressive virtual inertia saturate and

TABLE 1. Statistical analysis following a load shedding event. Frequency control in the case of non-railway consumption.

Cases	Gains (*Kp*, *Kv*)	Freq. deviation (mHz)		ROCOF (mHz/s)			Load				
							Power extrema (p.u.)		Energy (p.u. s)	Power derivative extrema (p.u./s)	
		Max.	RMS	Max.	Min.	RMS	Max.	Min.		Max.	Min.
Reference	0,0	131.9358	51.3609	375	-55.7522	51.0517	0.001176	0.001176	0.017644	0	0
Primary Control	0.2,0	131.6884	51.3119	375	-55.6087	50.9899	0.001400	0.001759	0.018361	0.0007	-0.0001
	0.4,0	131.4421	51.2631	375	-55.4674	50.9283	0.001622	0.001176	0.019077	0.0014	-0.0002
	0.6,0	131.1965	51.2145	375	-55.3257	50.8671	0.001844	0.001176	0.019793	0.0022	-0.0003
	0.8,0	130.9517	51.1661	375	-55.1848	50.806	0.002065	0.001176	0.020507	0.0029	-0.0004
	1.0,0	130.7077	51.1179	375	-55.0456	50.7453	0.002285	0.001176	0.021200	0.0036	-0.0005
Virtual Inertia	0,0.2	131.5725	51.3555	375	-54.8368	50.7788	0.002055	0.001044	0.017644	0.1175	-0.0018
	0,0.4	131.2533	51.3539	375	-54.0044	50.5895	0.002352	0.000917	0.017571	0.1866	-0.0035
	0,0.6	131.0644	51.3618	375	-53.3792	50.5321	0.002352	0.000792	0.017374	0.2792	-0.005
	0,0.8	130.9440	51.3732	375	-52.8714	50.5034	0.002352	0.000688	0.017143	0.2822	-0.0061
	0,1.0	130.8609	51.3864	375	-52.4304	50.4863	0.002352	0.000547	0.016896	0.2822	-0.0071
Combined control	0.8,0.2	130.5936	51.1608	375	-54.2808	50.5357	0.002309	0.001168	0.020508	0.1203	-0.0009
	0.6,0.4	130.6276	51.2148	375	-53.7569	50.4922	0.002352	0.001160	0.019638	0.1875	-0.0024
	0.4,0.6	130.7033	51.2717	375	-53.305	50.4893	0.002352	0.001151	0.018727	0.2798	-0.004
	0.2,0.8	130.7810	51.3289	375	-52.8637	50.487	0.002352	0.000861	0.017812	0.2822	-0.0056
	1,1	130.4023	51.1794	375	-52.9846	50.4627	0.002352	0.001135	0.020127	0.2822	-0.0042

decay faster. Those with high primary control remain with greater contributions once the maximum frequency deviation has passed, contrary to those with higher virtual inertia. In summary, a higher weight of primary frequency control enhances the behavior of frequency deviations, whereas a higher weight of virtual inertia improves response speed, which also reduces the time the VAC system is out of normal operation. However, much participation of virtual inertia control can impact negatively on frequency, saturate the VAC system, and require it to change drastically its operation point.

Beyond the previous qualitative analysis, Table 1 contains some statistics to evaluate the performance of controls during the studied period (between t= 220 s and t = 235 s): maximum value and root mean square (RMS) of frequency deviation, maximum and minimum values and RMS of ROCOF, maximum and minimum values of power and power derivative of the load, and the energy involved. Some conclusions are immediate: the greater the contribution of the controls, the lower the maximum frequency deviations; the minimum frequency deviation is identical for all cases due to the nature of the event; the maximum ROCOF is practically the same since the inertia of the system has not changed and due to the small actuation delay of controllers; and the higher the control gains, the more energy and power changes are required.

Fig. 7 compares some of the most important characteristics. It is noticeable that the primary control provides lower frequency deviations, and the virtual inertia provides lower

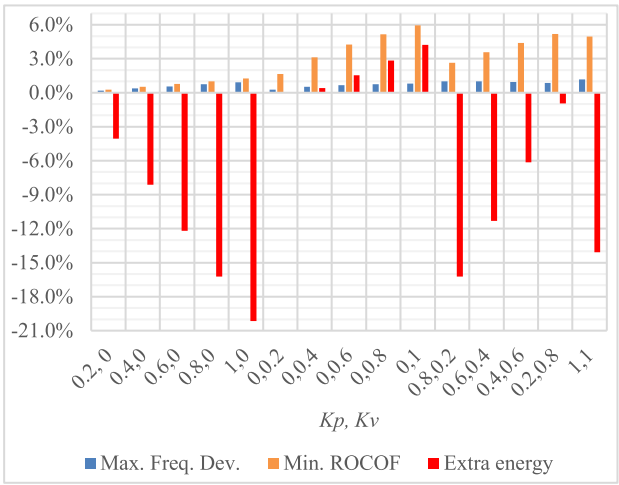

FIGURE 7. Reduction of main metrics with respect to the reference case.

frequency variations. However, the primary control demands an increase of net energy consumed, contrary to virtual inertia, where it is possible to reduce the net consumption. The combination allows to obtain the benefits of both controls without increasing energy consumption or constantly requiring sudden power variations. According to the results, under the scenario considered, it seems that a bit of virtual inertia with high primary frequency control ($K_p, K_v = 0.8,0.2$) can provide the third lowest frequency RMS, and the second

lowest maximum frequency deviation, although it consumes nearly 17% more energy than the reference case.

The following sections consider the railway consumption profile shown in [9]. The statistics are calculated during a multi-train circulation period when the power system faces a sudden load shedding or a generation losing. While trains are running, VAC systems are permitted to contribute to frequency control tasks by means of the abovementioned techniques.

B. CASE STUDY 2. RAILWAY CONSUMPTION. RESPONSE TO A SUDDEN LOAD SHEDDING

A fraction of the entire railway circulation (between $t = 220$ s and $t = 225$ s) is considered to show the contribution of railway VAC systems to frequency control. Also, the statistics are calculated in the same period to delimit the assessment to the showed period.

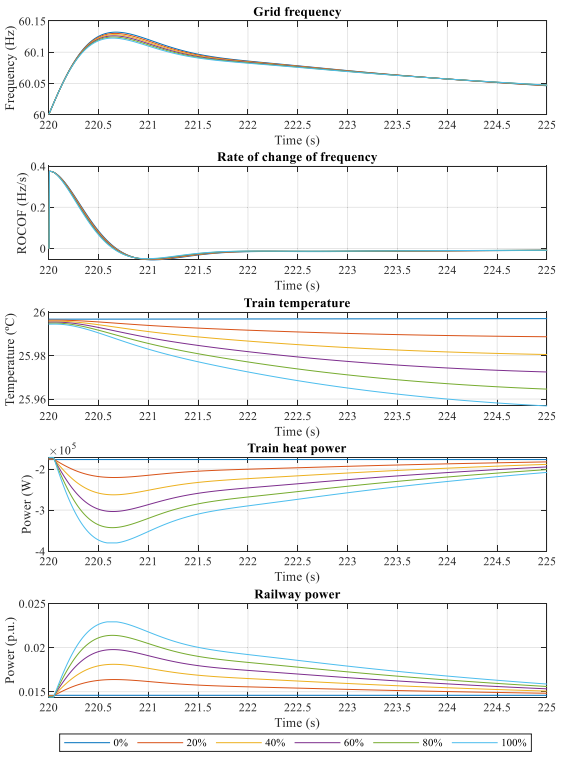

FIGURE 8. Primary frequency control response following a sudden load shedding. Variables of interest.

1) PRIMARY FREQUENCY CONTROL

Fig. 8 and Fig. 9 show the absolute results when implementing a control based on the instantaneous frequency deviations. At first, it is noticeable that more aggressive controls provide greater frequency reductions. Also, shorter times to reach maximum frequency values, greater increases in thermal power developed by the VAC system, and greater temperature deviations occur. By orienting the control to instantaneous frequency deviations, a direct improvement on ROCOF behavior is not achieved. Regardless the aggressiveness of

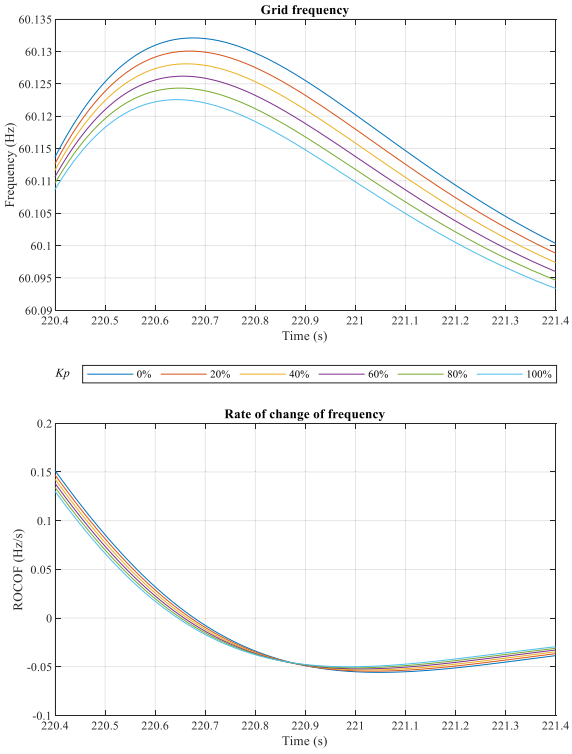

FIGURE 9. Primary frequency control response following a sudden load shedding. Zoom of frequency and rate of change of frequency.

the control, the variation in internal temperature is negligible. These results fully coincide with the ones in [9], where the possible contribution of trains to primary frequency control tasks, by means of their thermal inertia and VAC systems, is also assessed.

As mentioned in section IV-A, subtracting the reference case results (without VAC system participation on frequency control) from individual cases allows to scale figures toward a better visualization. Fig. 10 shows the same results of Fig. 8 but compared to the reference case. Apart from showing clearer behaviors, it allows to appreciate the order of magnitude of variations among cases. Here, a similar behavior to section IV-A primary frequency control case is obtained. The impact on thermal comfort, regardless of control aggressivity, is negligible. Also, the thermal inertia effect is appreciated. The temperature only decreased 0.04°C after almost five seconds of the maximum heat power injection.

2) VIRTUAL INERTIA CONTROL

Fig. 11 illustrates the behavior of the variables of interest in the case of implementing virtual inertia control, shown as their differences from those of the reference case. It is noticeable that varying VAC electric consumption proportionally to frequency variation rate also provides improvements in grid frequency deviations. However, the benefits are lower than the ones with primary frequency control. The main benefit of emulating inertia in frequency control lays on reducing

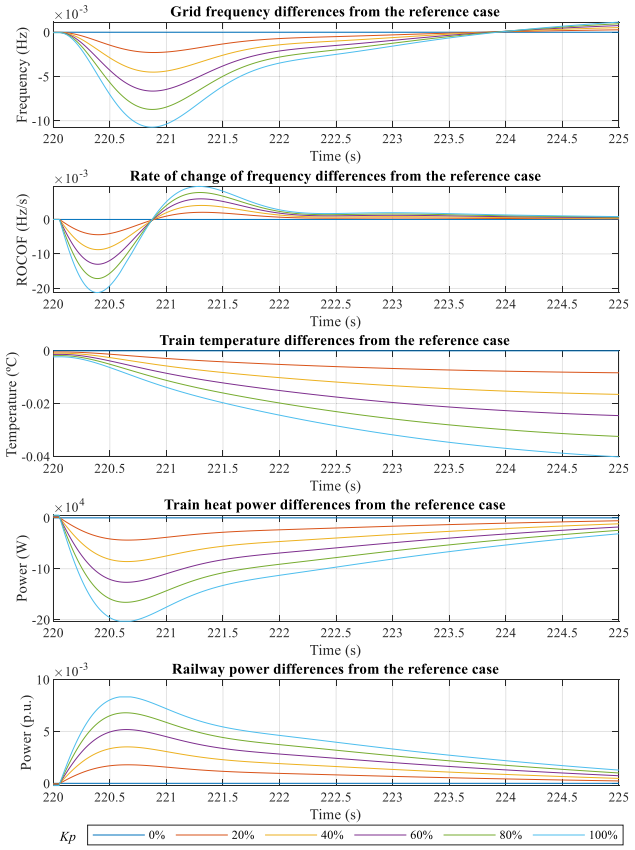

FIGURE 10. Primary frequency control response following a sudden load shedding. The reference case (without frequency control) has been subtracted from each case.

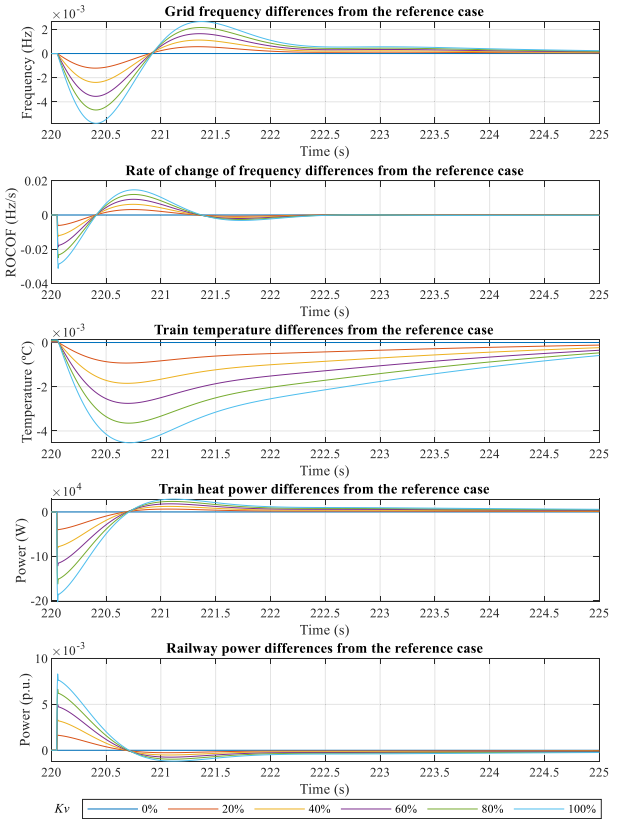

FIGURE 11. Virtual inertia control response following a sudden load shedding. The reference case (without frequency control) has been subtracted from each case.

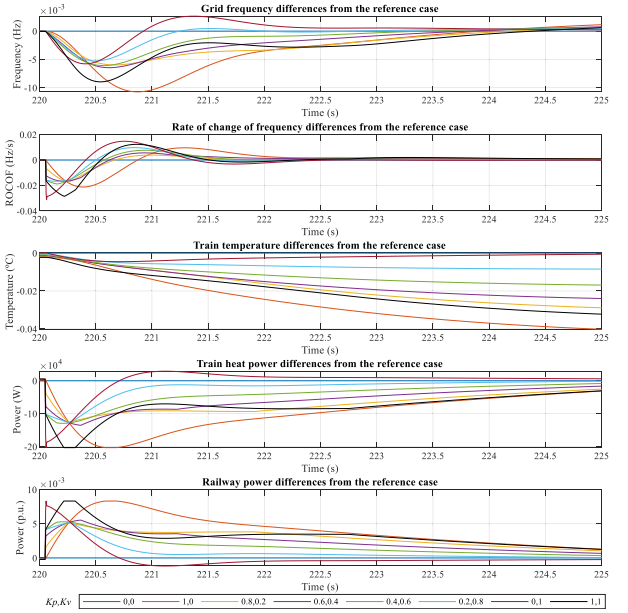

FIGURE 12. Combination of primary frequency and virtual inertia controls response following a sudden load shedding. The reference case (without frequency control) has been subtracted from each case.

the ROCOF. This requires lower maintained power during the event and lower air temperature variations (thousandth of degrees compared to hundredth of degrees in primary frequency control). As in the presented general study case, the maximum ROCOF does not vary, although there are improvements over time. In this circumstance, as the control is aimed to reduce the ROCOF, it is noteworthy that the more aggressive control, apart from requiring greater power variations, can also impact negatively on frequency deviation performance along time.

On thermal behaviors, under the same sudden load loss event, the VAC thermal power rapidly decreases and increases. Here the decrease was longer due to the resulting variation rate, which was imposed by the event nature. Also, the train temperature variations are negligible.

3) COMBINED CONTROL

With a combined control, the benefits and limitations of each individual control are present, as can be seen in Fig. 12. It is notable that no case risks thermal comfort, but their performances are significantly different in terms of frequency and power. The cases K_p, $K_v = (1,0)$ and K_p, $K_v = (0,1)$ present the slowest and the fastest frequency evolution, respectively, which are related to heat power. The extreme case K_p, $K_v = (1,1)$, which merges at 100% each controller, is the second best in reducing frequency deviations and variations, with approximately the average response time of the individual responses but saturating the power.

It is not clear which combination is more appropriate since the benefits in terms of frequency and thermal requirements are very similar. The selection of cases allows to notice how frequency and power behavior speed up along time with the increasement of virtual inertia and reduction of primary frequency control coefficients.

C. CASE STUDY 3. RAILWAY CONSUMPTION. RESPONSE TO A SUDDEN GENERATION LOSING

The following results were obtained with the same procedures as in the previous subsection, but this time a generation losing is studied. The event period and control settings are the same.

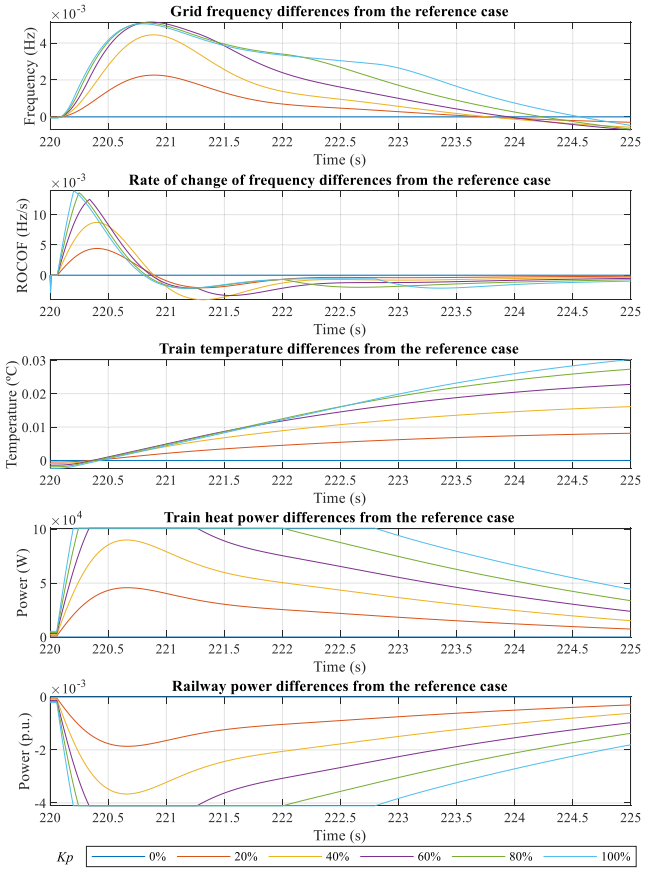

FIGURE 13. Primary frequency control response following a sudden generation losing. The reference case (without frequency control) has been subtracted from each case.

1) PRIMARY FREQUENCY CONTROL

Fig. 13 shows the results of primary frequency control following a sudden generation losing. Due to the decrease in generated power, there is a decrease in the thermal power delivered and, therefore, in the electrical power consumed by trains. Again, it is noticeable how the frequency deviations are mitigated depending on the aggressiveness of the control action. Similar to the results shown in [9], the control response saturates when reaching the technical minimum or maximum of thermal power delivered. The saturation time is inversely proportional to the control aggressivity. At saturation point, there are no extra benefits on increasing control aggressivity, but there are still high power requirements. Also, it can be seen how the saturation allows to maintain positive differences on frequency deviations, although it impacts on the normal drop of frequency deviations (first plot) and frequency variations (second plot). On thermal behavior, the little impact of varying VAC thermal power on thermal comfort is shown. It is also noticeable how the internal air train temperature behaves very similar in those cases where the frequency control saturates.

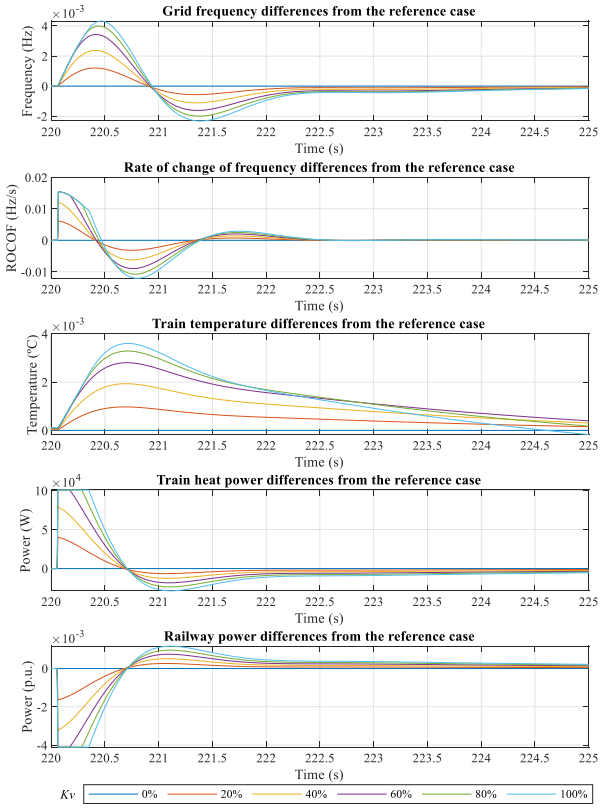

FIGURE 14. Virtual inertia control response following a sudden generation losing. The reference case (without frequency control) has been subtracted from each case.

2) VIRTUAL INERTIA CONTROL

Fig. 14 shows the responses of providing virtual inertia following a sudden generation losing. As in the previous section, increasing control aggressivity does not necessarily provide better system frequency deviation performance. In the ROCOF curve it is noticeable that greater aggressiveness allows its amplitude to decrease. However, due to heat power saturation, a virtual inertia coefficient of $K_v = 0.6$ would be enough to provide the maximum ROCOF reduction without demanding much power fluctuation and disturbing the overall frequency behavior.

From a frequency point of view, the primary control provides more benefits than the virtual inertia, even considering that some responses saturated. However, virtual inertia control allowed to achieve shorter power changes

than primary control during the same period, although power curves have larger slopes at the beginning. This also means that inner temperature deviations are insignificant.

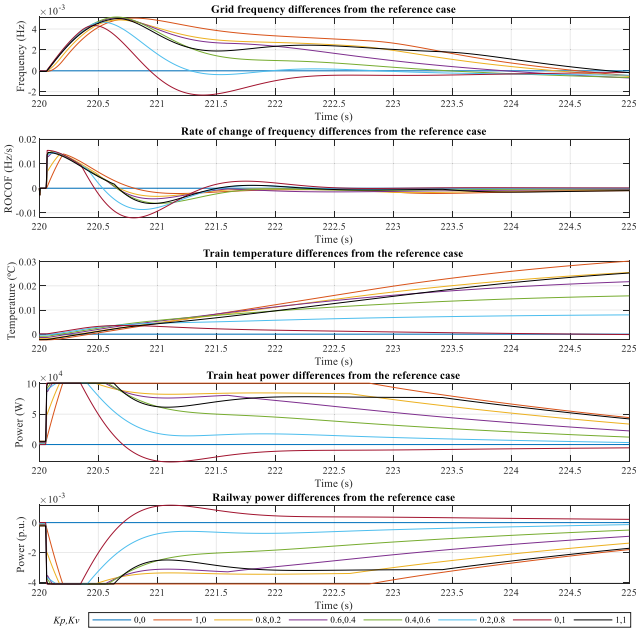

FIGURE 15. Combination of primary frequency and virtual inertia controls response following a sudden generation losing. The reference case (without frequency control) has been subtracted from each case.

3) COMBINED CONTROL

Fig. 15 shows the result of different combinations of primary control and virtual inertia following a sudden loss of generation. Regardless the combination of controls, there are always benefits in power system frequency performance. Again, it is noticeable how the benefits of both controls allow to minimize frequency deviations and ROCOF, and to maintain less technically demanding thermal power profiles than in the individual control scenarios.

At first, it is visible how the non-combined cases, K_p, $K_v = (1,0)$ and K_p, $K_v = (0,1)$, stablish the boundaries on every plot. This is, the case K_p, $K_v = (1,0)$ is the slowest and the one which mitigates frequency deviation the most, while the case K_p, $K_v = (0,1)$ is the opposite. However, the latter allows the fastest desaturation.

Since all cases reached saturation point, it is not clear which one performed the best. Nonetheless, the ''middle cases'', K_p, $K_v = (0.6,0.4)$ and K_p, $K_v = (0.4,0.6)$, seem to present an acceptable trade-off among contribution to frequency deviation reductions and power variations. This observation suggests maintaining a balance among primary frequency control and virtual inertia provision. Furthermore, the extreme case, K_p, $K_v = (1,1)$, despite saturation, also presents a balanced behavior, which is quite different from other cases. Pursuing a balanced combination of controls represents less technical requirement for VAC equipment and less energy consumption, while contributing approximately equally to frequency control.

D. GLOBAL RESULTS COMPARISON

Apart from the analysis of the previous figures, applying some statistics to the most relevant variables allows to evaluate the effectiveness of each control more precisely. This is especially necessary in the cases with control combinations, since in the individual cases all the responses have similar behaviors, but varying speed and amplitude depending on the aggressiveness of control. Then, the extrema and RMS values are calculated for the frequency deviation and its variation rate, considering the assigned values for each one (60 Hz and 0 Hz/s). Extrema, energy, and the extrema of its variation rate are also calculated for thermal power. Only the RMS value is calculated for the train inner air temperature deviation, based on 26°C.

1) STATISTICAL ANALYSIS OF THE RESPONSE TO A SUDDEN LOAD SHEDDING

Table 2 contains some statistics to evaluate primary frequency control, virtual inertia, and their combination in the scenario of sudden load shedding. In the primary control, what is observed in the graphs is corroborated. With greater aggressiveness, the maximum and minimum deviation decrease. The maximum undergoes a greater reduction because it is due to the load loss event, while the minimum is caused by the natural consumption of the railway. In addition, the RMS values allows observing the impact of each aggressiveness, where a maximum reduction of 3.8899 mHz is achieved. The effect of the primary control on the ROCOF is not negligible. The maximum ROCOF is imposed by the magnitude of the event and the inertia of the system, so it does not vary appreciably. The minimum ROCOF varies with greater rates than frequency deviation extrema. This depends on the normal railway consumption that is directly altered by the activation of the control. Even so, the difference between the frequency deviation and ROCOF RMS values is negligible. The effects of the primary control on the interior temperature are insignificant. However, in the developed thermal power, it is observed that a greater aggressiveness increases the minimum and reduces the maximum. The minimum increases due to the loss of load event, and the maximum decreases because the control requires following the frequency decrement caused by the natural consumption of the train during braking. Similarly, the variation rates of the thermal power grow up with the aggressiveness of control. Regarding energy consumption, an increase in total consumption with greater aggressiveness is appreciable. As expected, greater frequency deviations require more thermal power injection, and, therefore, more energy consumption.

According to virtual inertia implementation results, it is confirmed that it does manage to reduce the maximum and minimum frequency deviations, but to a lesser extent than the primary control. This can be appreciated in the fact that it provides higher RMS, maximum, and minimum values of frequency deviation than the primary control.

TABLE 2. Statistical analysis following a load shedding. Frequency control in railway consumption.

Cases	Gains (*Kp*, *Kv*)	Freq. deviation (mHz)			ROCOF (mHz/s)			Thermal power					Temperature deviation (°C)
								Extrema (MW)		Energy (kWh)	Extrema derivative (MW/s)		
		Max.	Min.	RMS	Max.	Min.	RMS	Max.	Min.		Max.	Min.	RMS
Ref.	0,0	132.096	1.1829	83.1319	375	-55.7833	87.2959	-0.17684	-0.17687	-0.2458	0	0	0.0031
Primary Control	0.2,0	130.0615	1.1733	82.3146	375	-54.5329	86.4113	-0.17578	-0.22057	-0.2743	0.0238	-0.1491	0.0088
	0.4,0	128.0934	1.1639	81.5181	375	-53.3368	85.5569	-0.1747	-0.26275	-0.3023	0.0467	-0.2982	0.0145
	0.6,0	126.1869	1.1548	80.7415	375	-52.1922	84.7312	-0.17364	-0.30347	-0.3297	0.0685	-0.4474	0.0201
	0.8,0	124.341	1.1458	79.9839	375	-51.0955	83.9328	-0.17259	-0.34281	-0.3565	0.0895	-0.5965	0.0256
	1.0,0	122.5563	1.1371	79.245	375	-50.0596	83.1613	-0.17156	-0.38	-0.3839	0.1097	-0.7456	0.0309
Virtual Inertia	0,0.2	131.4225	1.1828	83.1178	375	-54.055	86.418	-0.1704	-0.21758	-0.2463	0.1646	-8.1939	0.0035
	0,0.4	130.7685	1.1827	83.1043	375	-52.4121	85.5684	-0.16431	-0.25828	-0.2468	0.6033	-16.3865	0.004
	0,0.6	130.134	1.1826	83.0914	375	-50.8522	84.7459	-0.15856	-0.29898	-0.2474	1.3161	-24.5778	0.0045
	0,0.8	129.5174	1.1824	83.079	375	-49.3683	83.9492	-0.15312	-0.33968	-0.2479	2.3028	-32.7678	0.0049
	0,1.0	128.918	1.1823	83.067	375	-47.9585	83.1773	-0.14798	-0.38	-0.2484	3.4704	-40.9565	0.0054
Comb. control	0.8,0.2	126.126	1.1457	80.422	375	-51.9691	83.8376	-0.1726	-0.30256	-0.3436	0.086	-8.4445	0.0224
	0.6,0.4	125.7033	1.1545	80.8287	375	-50.6653	83.2956	-0.17366	-0.31218	-0.3276	0.1701	-16.3962	0.0199
	0.4,0.6	126.2488	1.1636	81.4813	375	-48.621	83.1557	-0.17473	-0.30617	-0.3038	0.1225	-24.4626	0.0155
	0.2,0.8	127.6854	1.1729	82.2868	375	-48.4458	83.6151	-0.17583	-0.30429	-0.2750	0.2316	-24.6239	0.0099
	1,1	123.8752	1.1369	80.1299	375	-46.3763	81.489	-0.17163	-0.38	-0.3543	0.3843	-25.6061	0.0247

Regarding the ROCOF, the contribution to the reduction of the minimum ROCOF is appreciated, which does not depend on the load loss event. However, the RMS value of the ROCOF is identical to that of the primary control, so there is no extra benefit in its application throughout the circulation of trains. The effects of virtual inertia on the interior temperature are lower than in primary control. It is noticeable that the RMS value is practically null and constant among cases with different control aggressiveness. Similarly, the power consumption is approximately equal to the case with no control implemented. However, the variation rate of the thermal power is considerably higher than the primary control. The application of this control demands a high-power variation capacity by the VAC equipment, which could be achieved through the activation of the compressor motors, fans or ventilators, circulation pumps, among other devices.

Regarding the results of the combination of the primary and virtual inertia controls, it is noticeable that it also manages to improve several parameters compared to the reference case. The combined control provided reductions in the maximum frequency deviation up to 8.2208 mHz, in the frequency RMS up to 3.00 mHz, and in the minimum ROCOF up to 9.407 mHz/s. The combination $K_p, K_v = (1,1)$ provided the second, first, third, first, and first best results on reducing maximum, minimum, and RMS value of frequency deviations, and the minimum and RMS value of ROCOF, respectively. Apart from this, it reduced the power fluctuation and the temperature deviation RMS.

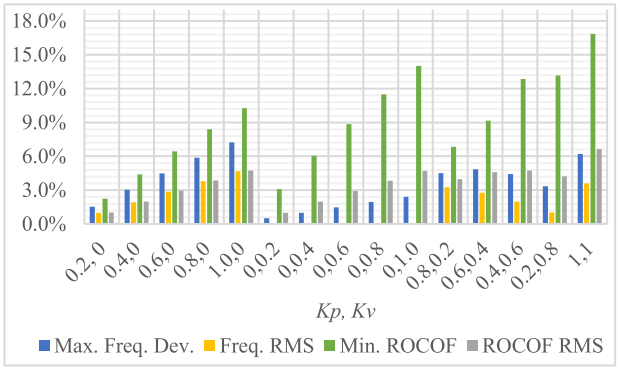

FIGURE 16. Reduction rates of relevant frequency-related variables following a load shedding.

In Fig. 16, the main differences regarding frequency deviations and ROCOF are easily appreciated. The primary control directly improves the maximum frequency deviations and, therefore, the RMS of frequency. It also reduces the minimum ROCOF and, on a lesser degree, the RMS of ROCOF. Virtual inertia reduces the maximum frequency deviations as well as the RMS of ROCOF but does not improve the RMS of frequency. Virtual inertia mainly reduces the minimum ROCOF. On the other hand, the

TABLE 3. Statistical analysis following a generation losing. Frequency control in railway.

Cases	Gains (*Kp*, *Kv*)	Freq. deviation (mHz)			ROCOF (mHz/s)			Thermal power					Temperature deviation (°C)
								Extrema (MW)		Energy (kWh)	Extrema (MW/s)		
		Max.	Min.	RMS	Max.	Min.	RMS	Max.	Min.		Max.	Min.	RMS
Ref.	0,0	1.4719	-131.792	82.897	72.3071	-375.058	88.3158	-0.17684	-0.17687	-0.2458	0	0	0.0031
Primary Control	0.2, 0	1.4598	-129.787	82.102	71.7121	-375.059	87.4454	-0.13114	-0.17577	-0.2147	0.1493	-0.0239	0.0032
	0.4,0	1.4479	-127.851	81.328	71.1305	-375.06	86.6067	-0.08694	-0.17469	-0.1841	0.2985	-0.0468	0.0083
	0.6,0	1.4363	-126.965	80.725	70.562	-375.06	86.082	-0.07600	-0.17363	-0.1583	0.4478	-0.06	0.0124
	0.8,0	1.425	-126.874	80.353	70.006	-375.061	85.8614	-0.07600	-0.17257	-0.1401	0.597	-0.0295	0.0148
	1.0,0	1.4139	-126.875	80.130	69.4621	-375.061	85.7473	-0.07600	-0.17154	-0.1279	0.7463	-0.0348	0.0159
Virtual Inertia	0,0.2	1.4718	-131.120	82.883	72.3012	-375.058	87.4515	-0.13614	-0.18339	-0.2454	8.4306	-0.1701	0.0026
	0,0.4	1.4717	-130.469	82.870	72.2953	-375.058	86.6173	-0.09540	-0.18945	-0.2449	16.8597	-0.6225	0.0022
	0,0.6	1.4715	-129.850	82.860	72.2893	-375.058	85.8888	-0.07600	-0.19518	-0.2447	20.1658	-0.2304	0.0019
	0,0.8	1.4714	-129.364	82.871	72.2834	-375.058	85.54	-0.07600	-0.20044	-0.2455	18.8146	-0.3196	0.0019
	0,1.0	1.4713	-128.997	82.896	72.2774	-375.058	85.3459	-0.07600	-0.20543	-0.2469	17.4619	-0.396	0.002
Comb. control	0.8,0.2	1.4248	-126.928	80.547	69.9983	-375.061	85.4226	-0.07600	-0.17258	-0.1468	8.7289	-0.07	0.0134
	0.6,0.4	1.436	-126.750	80.860	70.5475	-375.06	85.1455	-0.07600	-0.17365	-0.1623	16.8539	-0.1927	0.0117
	0.4,0.6	1.4475	-126.661	81.363	71.11	-375.059	84.9949	-0.07600	-0.17472	-0.1853	16.7537	-0.1302	0.0085
	0.2,0.8	1.4592	-127.679	82.110	71.6864	-375.059	85.1335	-0.07600	-0.17582	-0.2156	15.9726	-0.2462	0.0035
	1,1	1.4131	-126.795	80.616	69.4279	-375.061	85.1499	-0.07600	-0.17158	-0.1461	12.7257	-0.2288	0.0125

combination of both controls allows to enhance the overall frequency behavior. It almost entirely combines the benefits of individual controls.

2) STATISTICAL ANALYSIS OF THE RESPONSE TO A SUDDEN GENERATION LOSING

Table 3 contains some statistics to evaluate the primary control, the virtual inertia, and their combination in the scenario of a sudden loss of generation. The results of the primary frequency control support what was obtained in the previous cases. It is clearly observable that the aggressiveness of the control provides greater reductions of both frequency deviation extrema and, therefore, the RMS value. It affects the extrema and RMS of ROCOF at similar rates. The energy consumption due to the injection of thermal power also decreased with the increase of the aggressiveness of the control. The extrema of thermal powers, as well as their variation rate, also increased. The temperature of the interior air, although it has small variations compared to its nominal value, varied more noticeably when faced with higher aggressiveness.

Regarding the virtual inertia, it is also possible to reduce the extrema of the frequency deviations and their RMS values, although to a lesser degree. The virtual inertia did not have notable benefits on reducing ROCOF extrema but did reduce the ROCOF RMS more than primary control. The energy consumption, and the temperature deviation RMS varied minimally according to control aggressiveness, as it happened in the load shedding scenario. Furthermore, like the previous scenario, it is notable how the aggressiveness of the virtual inertia imposes greater variations of the thermal power to be injected.

The combination of both controls, comparing the cases with same K_p, K_v does provide greater reductions in the extrema of frequency deviations. In addition, it allows obtaining lower RMS of ROCOF compared to the application of both controls individually. However, in the RMS of frequency and energy consumption, the combined controls improved virtual inertia results, but they were similar to primary control ones. The deviations of the internal temperature remain negligible. Again, the combination of both controls also requires lower sudden variations in thermal power, although in this scenario the benefit obtained is lower.

Fig. 17 shows some of the parameters that varied most markedly between the different combinations of controls in the face of sudden generation loss. The extrema of frequency deviations and the RMS of frequency and ROCOF were selected. According to what was previously visualized, the virtual inertia applied individually does not represent benefits in any variable, compared to the individual primary control scenario and the combination of both. The primary control individually provides similar reductions, to the combination of the controls, of the lower limit of the frequency deviations, as the RMS of frequency is also similar. However, combining the controls (primary and virtual inertia) does provide greater

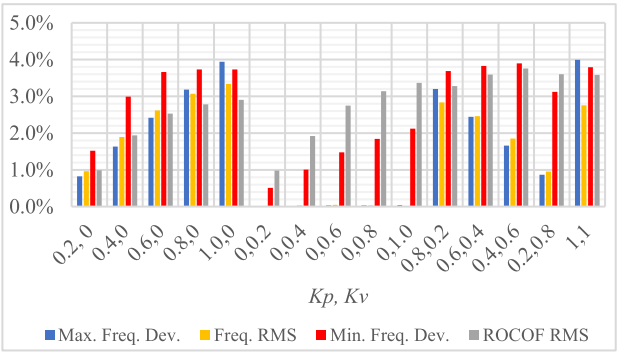

FIGURE 17. Reduction rates of relevant frequency-related variables following a generation losing.

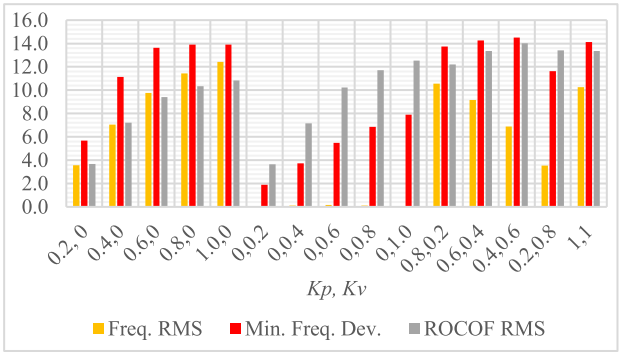

FIGURE 19. Relative impact index (%/p.u.) of relevant frequency-based variables following a generation losing.

benefits in the RMS of ROCOF and in the reduction of the maximum frequency deviations, while requiring lower thermal power variations than a standalone virtual inertia control.

3) RELATIVE IMPACT INDEX

To better appreciate the contribution of VAC systems of trains to frequency control, the size of the controllable load should be taken into account. In the case considered, a maximum power of 0.0013 p.u. per train is available for frequency control tasks. Although the number of trains varies over time, it can be stated that a total maximum load of 0.0052 p.u. provided the prior benefits in a 2.0 p.u. system (four trains and two generators). The objective of the presented approach is not to completely handle the frequency deviations by itself, but to be just one of many contributors. To better assess the benefits of its contribution, this section shows relative results, compared to load size. This is calculated by dividing some of the most relevant results (percentage reduction) by the total maximum available load (power capacity in p.u.).

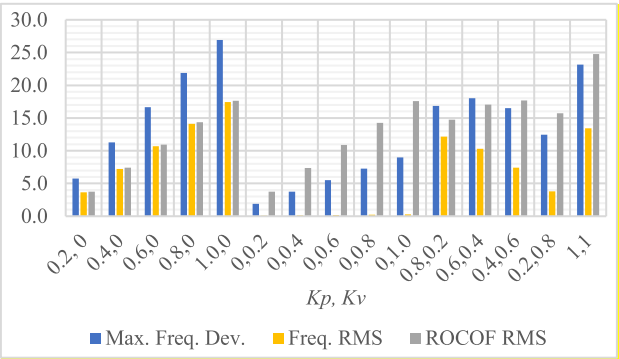

FIGURE 18. Relative impact index (%/p.u.) of relevant frequency-related variables following a load shedding.

Fig. 18 and Fig. 19 show the relative impact index following a load shedding and a generation losing, respectively. In both situations, the percentage reductions of RMS of frequency and ROCOF are calculated. Due to the diverse nature of each situation, the relevant statistics to be reduced are different. In the case of load shedding, maximum frequency deviation is expected to increase and it is included in Fig. 18. In the generation losing case, the same behavior is expected but with minimum frequency deviation, and it is included in Fig. 19.

The previous figures show the same strong relations of primary frequency control with frequency RMS, and virtual inertia with ROCOF RMS. In addition, the results indicate how large could be the reductions if more loads (up to 1.0 p.u.) apply similar frequency controls. Depending on the gain of controllers, the frequency performance improvement can be even more relevant. For example, in Fig. 18, the possibility of reducing up to 27%, 17%, and 25% the maximum frequency deviation, frequency RMS, and ROCOF RMS, respectively, can be seen. In Fig. 19, a maximum possible reduction of 12%, 14%, and 14% in frequency RMS, minimum frequency deviation, and ROCOF RMS, respectively, is showed.

V. DISCUSSION

The integration of non-conventional generation technologies has required the electrical energy systems to adapt to continue providing security, stability, and power quality in the energy supply. For this reason, research has been carried out around the world on how these new technologies, and other participants in the sector, can contribute to maintain the integrity of electrical power systems.

Thus, the contribution of the different types of demand has been studied so that they participate in the ancillary services of power systems, reduction of congestion on lines, or optimum economic consumption, among other aspects.

The relation between the total railway consumption and the fraction related to VAC systems, the power system characteristics, and the magnitude of the event largely define the relevance of railway contribution to frequency control. Even a small relative variation of consumption can impact positively on frequency control if the railway, and the associated VAC systems, are a significant load in the instantaneous grid power balance.

The result section shows how the control action affects the minimum ROCOF following a load shedding event (up to 16.86% reduction), and slightly impacts on its maximum

value following a generation losing event (up to 3.98% reduction). These values depend on power system inertia, which does not vary, and on the instantaneous power balance. In the model, the VAC system consumption is considerable smaller than the power involved in the event and the train traction consumption. Therefore, following a load shedding event, its magnitude defines the maximum ROCOF, while the minimum ROCOF is still defined by the normal power consumption (traction and auxiliaries). This explains why the railway frequency control only improved the minimum. In a generation losing situation, the event magnitude defines the minimum ROCOF, while the maximum ROCOF is still defined by the normal power consumption (braking and auxiliaries). Since, during braking, the power exchange between railway and grid is minimum (no injection of regenerative braking energy and auxiliaries' consumption) the influence on frequency performance of varying VAC system consumption is going to be also minimum. In conclusion, the possible benefits on frequency control can considerably vary depending on the type of event in the power system.

The VAC operation status, prior to the activation of the frequency control, limits its contribution due to operating boundaries. It has been shown that the frequency deviations and variations demand amounts of thermal power that tend to saturate the VAC system, especially in the case of generation loss, where the lower limit is reached several times. In the case of a sudden load shedding, if the VAC is handling a large thermal load (passengers, solar radiation, etc.), it is not possible to increase much more its electrical consumption to mitigate the increase in frequency. Similarly in case of sudden loss of generation, the VAC contribution could be minimal if the previous instantaneous thermal load is low compared to its rated power. Regardless the situation, it has been proven that the thermal comfort of passengers is not compromised.

On the other hand, the benefits of applying these control techniques should consider the VAC system technical requirements. In addition to the reductions on frequency deviations and ROCOF, there are also reductions on the delivered thermal power and, therefore, on electrical consumption. However, these benefits require the capacity of providing sudden thermal power changes, especially on virtual inertia cases, where reductions of some millihertz demand variations of several megawatts per second in the VAC system operation. Therefore, the doable contribution of train VAC systems also depends on their operation ranges. Some of the benefits of combining primary frequency control and virtual inertia, besides the improvement on frequency performance, is the reduction of technical requirements while achieving better frequency performance. Hence, VAC system fatigue, and other possible issues, can be mitigated. It is also worth mentioning that controls do not combine linearly, even if the implemented equation does. The action of one control can affect the performance of the other one. Then, an appropriate adaptive combination over time could allow to obtain even more benefits.

The presented work is the first levels of technology readiness. Future development toward real-life applications will include laboratory experiments and validation. Some possible challenges can be related to: the VAC systems' own dynamics, the actual implementation of their control systems, and measurement and transmission of grid frequency signal, among others.

VI. CONCLUSION

The present work is focused on expanding the contribution of railway systems to frequency control tasks. There are few studies where the railway infrastructure is considered as a manageable load and even fewer studies where they participate in the ancillary services of power systems. The main contribution of this work is to propose that the trains contribute to primary frequency control and to the provision of virtual inertia, by using the thermal inertia of wagons via their HVAC systems.

The results of the case studies allow to appreciate the possible positive effects:

- It is observed how maximum and minimum frequency deviations and ROCOF are mitigated in different proportions depending on the aggressiveness of the control. Up to 7.22%, 3.89%, 3.98%, and 16.86% absolute reduction among all cases and control combinations, respectively.
- Increasing control aggressiveness also demands more VAC system power variation capacity, especially in the application of virtual inertia where thermal power rates increase markedly. Because of this, the operational limits and dynamics of VAC systems will largely determine how much trains could contribute to frequency control tasks. Maximum heat power is reached in cases where K_p or $K_v = 1$.

TABLE 4. Parameters' values and specifications.

Parameters (units)	Values
Generators inertia (s)	4.0
Generators dead band (mHz)	±1
Generators PI controller gains	-20, -5
Load damping factor (%)	1
Base power (MW)	18
Train weight (kg)	204525
Train power conversion efficiency (%)	95
Davis coefficients (N, Nh/km, Nh^2/km^2)	2547.648, 21.6048, 0.59
Train length, width, and height (m)	86.094, 2.71, 3.859
Dwelling and headway times (s)	30.0, 120.0
HVAC system PI controller gains	50, 1
HVAC system frequency control dead band (mHz)	±17
Maximum solar irradiance (W/m^2)	760
Outside air temperature (°C)	30
Thermal envelope characteristics	See 11^{th} configuration in [9]

- Likewise, measuring the rate of variation of thermal power would allow estimating the degree of fatigue these devices are exposed to.

APPENDIX A

See Table 4.

ACKNOWLEDGMENT

The authors would like to thank the company ''Metro de Panamá'' and ''Universidad Tecnológica de Panamá'' for providing the information of Panama Metro Line 1.

REFERENCES

[1] L. Meegahapola, P. Mancarella, D. Flynn, and R. Moreno, ''Power system stability in the transition to a low carbon grid: A techno-economic perspective on challenges and opportunities,'' *WIREs Energy Environ.*, vol. 10, no. 5, pp. 1–27, Sep. 2021, doi: 10.1002/wene.399.

[2] H. H. Alhelou, M. E. Hamedani-Golshan, R. Zamani, E. Heydarian-Forushani, and P. Siano, ''Challenges and opportunities of load frequency control in conventional, modern and future smart power systems: A comprehensive review,'' *Energies*, vol. 11, no. 10, p. 35, 2018, doi: 10.3390/en11102497.

[3] M. Ramesh, A. K. Yadav, and P. K. Pathak, ''An extensive review on load frequency control of solar-wind based hybrid renewable energy systems,'' *Energy Sources A, Recovery, Utilization, Environ. Effects*, Jun. 2021, doi: 10.1080/15567036.2021.1931564.

[4] M. Pierro, R. Perez, M. Perez, D. Moser, and C. Cornaro, ''Imbalance mitigation strategy via flexible PV ancillary services: The Italian case study,'' *Renew. Energy*, vol. 179, pp. 1694–1705, Dec. 2021, doi: 10.1016/j.renene.2021.07.074.

[5] S. Padhy and S. Panda, ''Simplified grey wolf optimisation algorithm tuned adaptive fuzzy PID controller for frequency regulation of interconnected power systems,'' *Protection Control Mod. Power Syst.*, vol. 43, no. 1, pp. 4089–4101, 2022, doi: 10.1080/01430750.2021.1874518.

[6] H. Rezk, M. A. Mohamed, A. A. Z. Diab, and N. Kanagaraj, ''Load frequency control of multi-interconnected renewable energy plants using multi-verse optimizer,'' *Comput. Syst. Sci. Eng.*, vol. 37, no. 2, pp. 219–231, 2021, doi: 10.32604/csse.2021.015543.

[7] M. Hussain and Y. Gao, ''A review of demand response in an efficient smart grid environment,'' *Electr. J.*, vol. 31, no. 5, pp. 55–63, Jun. 2018, doi: 10.1016/j.tej.2018.06.003.

[8] W. Huang, N. Zhang, C. Kang, M. Li, and M. Huo, ''From demand response to integrated demand response: Review and prospect of research and application,'' *Protection Control Mod. Power Syst.*, vol. 4, no. 1, p. 13, Dec. 2019, doi: 10.1186/s41601-019-0126-4.

[9] J. Araúz and S. Martinez, ''Contribution of the thermal inertia of trains to the primary frequency control of electric power systems,'' *Sustain. Energy, Grids Netw.*, vol. 34, Jun. 2023, Art. no. 100988, doi: 10.1016/j.segan.2022.100988.

[10] U. Tamrakar, D. Shrestha, M. Maharjan, B. P. Bhattarai, T. M. Hansen, and R. Tonkoski, ''Virtual inertia: Current trends and future directions,'' *Appl. Sci.*, vol. 7, no. 7, pp. 1–29, 2017, doi: 10.3390/app7070654.

[11] J. Fang, H. Li, Y. Tang, and F. Blaabjerg, ''On the inertia of future more-electronics power systems,'' *IEEE J. Emerg. Sel. Topics Power Electron.*, vol. 7, no. 4, pp. 2130–2146, Dec. 2019, doi: 10.1109/JESTPE.2018.2877766.

[12] T. Chen, J. Guo, B. Chaudhuri, and S. Y. Hui, ''Virtual inertia from smart loads,'' *IEEE Trans. Smart Grid*, vol. 11, no. 5, pp. 4311–4320, Sep. 2020, doi: 10.1109/TSG.2020.2988444.

[13] H. Yang, T. Li, Y. Long, C. L. P. Chen, and Y. Xiao, ''Distributed virtual inertia implementation of multiple electric springs based on model predictive control in DC microgrids,'' *IEEE Trans. Ind. Electron.*, vol. 69, no. 12, pp. 13439–13450, Dec. 2022, doi: 10.1109/TIE.2021.3130332.

[14] W. Hao and Z. Chen, ''An improved virtual capacitor control strategy for DC electric railway system,'' in *Proc. IEEE Southern Power Electron. Conf. (SPEC)*, Dec. 2021, pp. 1–6, doi: 10.1109/SPEC52827.2021.9709468.

[15] W. Yu, Z. Liu, and I. A. Tasiu, ''Virtual inertia control strategy of traction converter in high-speed railways based on feedback linearization of sliding mode observer,'' *IEEE Trans. Veh. Technol.*, vol. 70, no. 11, pp. 11390–11403, Nov. 2021, doi: 10.1109/TVT.2021.3112827.

[16] D. Ochoa and S. Martinez, ''Contribución de los aerogeneradores de velocidad variable al control primario de frecuencia en sistemas de energía eléctrica,'' Ph.D. thesis, Dept. Elect. Eng., Universidad Politécnica de Madrid, Madrid, Spain, 2019. [Online]. Available: http://oa.upm.es/56530/, doi: 10.20868/UPM.thesis.56530.

[17] K. Almaksour, Y. Krim, N. Kouassi, N. Navarro, B. François, T. Letrouvé, C. Saudemont, L. Taunay, and B. Robyns, ''Comparison of dynamic models for a DC railway electrical network including an AC/DC bi-directional power station,'' *Math. Comput. Simul.*, vol. 184, pp. 244–266, Jun. 2021, doi: 10.1016/j.matcom.2020.05.027.

[18] H. Alnuman, D. Gladwin, and M. Foster, ''Electrical modelling of a DC railway system with multiple trains,'' *Energies*, vol. 11, no. 11, p. 3211, Nov. 2018, doi: 10.3390/en11113211.

[19] S. Su, T. Tang, and Y. Wang, ''Evaluation of strategies to reducing traction energy consumption of metro systems using an optimal train control simulation model,'' *Energies*, vol. 9, no. 2, pp. 1–19, 2016, doi: 10.3390/en9020105.

[20] R. Mathew, F. Flinders, and W. Oghanna, ''Locomotive 'total systems' simulation using SIMULINK,'' in *Proc. Int. Conf. Electr. Railways United Eur.*, no. 405, 1995, pp. 202–206, doi: 10.1049/cp:19950207.

[21] C. S. Chang, A. Khambadkone, and Z. Xu, ''Modeling and simulation of DC transit system with VSI-fed induction motor driven train using PSB/MATLAB,'' in *Proc. 4th IEEE Int. Conf. Power Electron. Drive Syst.*, vol. 2, Oct. 2001, pp. 881–885, doi: 10.1109/peds.2001.975436.

[22] F. Du, J. H. He, L. Yu, M. X. Li, Z. Q. Bo, and A. Klimek, ''Modeling and simulation of metro DC traction system with different motor driven trains,'' in *Proc. Asia–Pacific Power Energy Eng. Conf.*, 2010, pp. 5–8, doi: 10.1109/APPEEC.2010.5448372.

[23] A. Capasso, R. Lamedica, A. Ruvio, M. Ceraolo, and G. Lutzemberger, ''Modelling and simulation of electric urban transportation systems with energy storage,'' in *Proc. IEEE 16th Int. Conf. Environ. Electr. Eng. (EEEIC)*, Jun. 2016, pp. 1–5, doi: 10.1109/EEEIC.2016.7555480.

[24] L. Yang, X. Li, and J. Tu, ''Thermal comfort analysis of a high-speed train cabin considering the solar radiation effects,'' *Indoor Built Environ.*, vol. 29, no. 8, pp. 1101–1117, Oct. 2020, doi: 10.1177/1420326X19876082.

[25] S. Istomin and A. Shtraukhman, ''Simulation model of the heating and air conditioning system of DC electric trains,'' in *Proc. E3S Web Conf.*, vol. 135, 2019, p. 9, doi: 10.1051/e3sconf/201913502018.

[26] R. Mastrullo, A. W. Mauro, and C. Vellucci, ''Refrigerant alternatives for high speed train A/C systems: Energy savings and environmental emissions evaluation under variable ambient conditions,'' *Energy Proc.*, vol. 101, pp. 280–287, Nov. 2016, doi: 10.1016/j.egypro.2016.11.036.

[27] W. Pan, S. C. Dhulipala, and A. S. Bretas, ''A distributed approach for DG integration and power quality management in railway power systems,'' in *Proc. 17th IEEE Int. Conf. Environ. Electr. Eng. IEEE Ind. Commercial Power Syst. Eur. (EEEIC/ICPS Europe)*, Jun. 2017, pp. 1–6, doi: 10.1109/EEEIC.2017.7977714.

[28] N. Li, L. Yang, X. Li, X. Li, J. Tu, and S. C. P. Cheung, ''Multi-objective optimization for designing of high-speed train cabin ventilation system using particle swarm optimization and multi-fidelity kriging,'' *Building Environ.*, vol. 155, pp. 161–174, May 2019, doi: 10.1016/j.buildenv.2019.03.021.

[29] J. A. Thompson, G. G. Maidment, and J. F. Missenden, ''Modelling low-energy cooling strategies for underground railways,'' *Appl. Energy*, vol. 83, no. 10, pp. 1152–1162, Oct. 2006, doi: 10.1016/j.apenergy.2005.12.001.

[30] K. Jenkins, M. Gilbey, J. Hall, V. Glenis, and C. Kilsby, ''Implications of climate change for thermal discomfort on underground railways,'' *Transp. Res. D, Transp. Environ.*, vol. 30, pp. 1–9, Jul. 2014, doi: 10.1016/j.trd.2014.05.002.

[31] R. N. Hofstädter, T. Zero, C. Dullinger, G. Richter, and M. Kozek, ''Heat capacity and heat transfer coefficient estimation for a dynamic thermal model of rail vehicles,'' *Math. Comput. Model. Dyn. Syst.*, vol. 23, no. 5, pp. 439–452, Sep. 2017, doi: 10.1080/13873954.2016.1263670.

[32] I. M. Alotaibi, M. A. Abido, and M. Khalid, ''Primary frequency regulation by demand side response,'' *Arabian J. Sci. Eng.*, vol. 46, no. 10, pp. 9627–9637, Oct. 2021, doi: 10.1007/s13369-021-05440-x.

[33] S. Williams, M. Short, and T. Crosbie, "On the use of thermal inertia in building stock to leverage decentralised demand side frequency regulation services," *Appl. Thermal Eng.*, vol. 133, pp. 97–106, Mar. 2018, doi: 10.1016/j.applthermaleng.2018.01.035.
[34] Y. Zhou, H. Bi, H. Wang, Y. Zhao, and B. Lei, "Time-delay characteristics of air-conditioning system for subway trains," *J. Building Eng.*, vol. 40, Aug. 2021, Art. no. 102731, doi: 10.1016/j.jobe.2021.102731.
[35] E. Trygstad, "R744 HVAC unit for NSB flirt trains," M.S. thesis, Dept. Energy Process Eng., Norwegian Univ. Sci. Technol., Trondheim, Norway, 2017.
[36] I. Beil, I. Hiskens, and S. Backhaus, "Frequency regulation from commercial building HVAC demand response," *Proc. IEEE*, vol. 104, no. 4, pp. 745–757, Apr. 2016, doi: 10.1109/JPROC.2016.2520640.
[37] M. H. Moradi and F. Amiri, "Virtual inertia control in islanded microgrid by using robust model predictive control (RMPC) with considering the time delay," *Soft Comput.*, vol. 25, no. 8, pp. 6653–6663, Apr. 2021, doi: 10.1007/s00500-021-05662-z.
[38] X. Hou, Y. Sun, X. Zhang, J. Lu, P. Wang, and J. M. Guerrero, "Improvement of frequency regulation in VSG-based AC microgrid via adaptive virtual inertia," *IEEE Trans. Power Electron.*, vol. 35, no. 2, pp. 1589–1602, Feb. 2020, doi: 10.1109/TPEL.2019.2923734.
[39] D. Ochoa and S. Martinez, "Proposals for enhancing frequency control in weak and isolated power systems: Application to the wind-diesel power system of San Cristobal Island–Ecuador," *Energies*, vol. 11, no. 4, p. 25, 2018, doi: 10.3390/en11040910.
[40] M. Khan, H. Sun, Y. Xiang, and D. Shi, "Electric vehicles participation in load frequency control based on mixed H_2/H∞," *Int. J. Electr. Power Energy Syst.*, vol. 125, Feb. 2021, Art. no. 106420, doi: 10.1016/j.ijepes.2020.106420.
[41] G. Benysek, J. Bojarski, R. Smolenski, M. Jarnut, and S. Werminski, "Application of stochastic decentralized active demand response (DADR) system for load frequency control," *IEEE Trans. Smart Grid*, vol. 9, no. 2, pp. 1055–1062, Mar. 2018, doi: 10.1109/TSG.2016.2574891.
[42] Red Eléctrica de España. (2006). *Establecimiento de la Reserva Para la Regulación Frecuencia-Potencia, Boletín Oficial del Estado N°173*. Accessed: Feb. 15, 2022. [Online]. Available: https://www.ree.es/sites/default/files/01_ACTIVIDADES/Documentos/ProcedimientosOperacion/RES_PO_1.5.pdf
[43] D. Ochoa and S. Martinez, "Frequency control issues in power systems: The effect of high share of wind energy," *IEEE Latin Amer. Trans.*, vol. 16, no. 7, pp. 1934–1944, Jul. 2018, doi: 10.1109/TLA.2018.8447360.
[44] Z. He, C. Wan, and Y. Song, "Frequency regulation from electrified railway," *IEEE Trans. Power Syst.*, vol. 37, no. 3, pp. 2414–2431, May 2022, doi: 10.1109/TPWRS.2021.3119706.

JESÚS ARAÚZ was born in Panama, in 1996. He received the B.S. degree in electromechanical engineering from Universidad Tecnologica de Panama (UTP), Panama City, Panama, in 2020, and the M.S. degree in electrical engineering from Universidad Politecnica de Madrid (UPM), Madrid, Spain, in 2022, where he is currently pursuing the Ph.D. degree in electrical and electronics engineering. His research interests include energy efficiency in buildings, railway systems, electrical generation from renewable energy, and ancillary services in power systems.

SERGIO MARTINEZ (Senior Member, IEEE) was born in Spain, in 1969. He received the M.S. degree in industrial engineering and the Ph.D. degree in electrical engineering from Universidad Politecnica de Madrid (UPM), Madrid, Spain, in 1993 and 2001, respectively. He is currently an Associate Professor with the Department of Electrical Engineering, UPM. His research interests include electrical generation from renewable energy and the provision of ancillary services from electrical equipment connected to power systems through power electronics.